Fluid Dynamics Analysis of Fish Aggregation Device using Particle Image Velocimetry

Kyounghoon Lee[1], Sung Il Lee[2] and Doo Nam Kim[2]

[1]School of Marine Technology, Chonnam National University, Yeosu 59626, Rep. of Korea
[2]Distant Water Fisheries Resources Research Division, National Institute of Fisheries Science, Busan 46083, Rep. of Korea

Abstract

In the process of developing a fish aggregating device (FAD) for reducing the entanglement of bycatch, the flows that occur in both existing high-risk net-type entangling FADs and low-risk rope-type FADs equipped with non-entangling cloth attractors were measured using a flow visualization technique. At an inlet velocity of 0.504 m/s, the mean velocity data for net and rope FADs were 0.525 m/s and 0.280 m/s, respectively, and the turbulence intensity data were measured as 10.8% and 46.9%, respectively. The mean velocity data for the rope FAD and spindle-type fish were 0.126 m/s and 0.164 m/s, respectively, and the turbulence intensity data were 37.0% and 17.9% respectively, at an inlet velocity of 0.2 m/s. For the measurement and analysis of the flow data, the particle image velocimetry method was used. The flow velocity and turbulence intensity data revealed that compared to existing net-type entangling FADs, rope-type FADs equipped with ribbons had a significantly larger or smaller difference in the velocity and turbulence intensity compared to the surrounding flow rate.

Introduction

There are a variety of different methods used in the fishing industry that exploit biological characteristics such as phototaxis, stereotaxis, and phonotaxis. However, phototaxis is the most commonly used method, and numerous studies have focused on this approach (An et al., 2012). Seine fishery is the most representative type that is used in open sea, with tuna as the major target species. Tuna are attracted to driftwood through phototaxis (Moon et al., 1996, 2007).

As a plan to conserve fish resources in Korea, an artificial reef project began in 1971 to improve the environment of their habitat. As a result, huge investments were made to create artificial reefs for breeding fish (Lee, 2000).

To create habitats for mackerel, amberjack, and bonito, which only respond to fluid stimuli such as the topographic waves generated above reefs, the structure of the artificial reef was designed to embrace the fluid stimuli at its surface and middle layers. These reefs were built to be taller than the average reef and designed to block flows, generate fluid sounds, and shelter flows.

To prove the effectiveness of stereotaxis in attracting fish based on fluid stimuli with tuna, which are the target species of the FAD, the fluid characteristics of existing net-type FADs, rope-type FADs, and spindle-type fish were quantitatively analyzed using flow velocity and turbulence intensity through a flow visualization technique.

Material and Methods

For the flow visualization measurement, a particle image velocimetry (PIV) camera (ES 4.0, Kodak, USA), Nd:YAG laser (200 mJ,15 Hz, ESI, USA), PIV software

(Thinkers EYES 2D, TNTech, Korea), particles (silver-coated glass spheres, Dantec, Germany), and a PC (i7, Intel, Korea) were used. The inlet velocity was 0.504 m/s and the measurement area was 200 mm (width) × 200 mm (height). The same equipment was used for the spindle fish, with an inlet velocity of 0.2 m/s, and the measurement range of 200 mm (width) × 150 mm (height). The measured data were compared with the net-type FAD data. The PIV technique is a method of analyzing particle behavior using digital visualization after the introduction of particles with the same mass as the medium of the flow field. The PIV technique, which is a non-contact method of flow measurement, is effective when contact-type sensors are difficult to install and a variety of different flow fields are formed. The technique is effective in analyzing the flow surrounding the subject of interest when the analysis requires multi-point measurements.

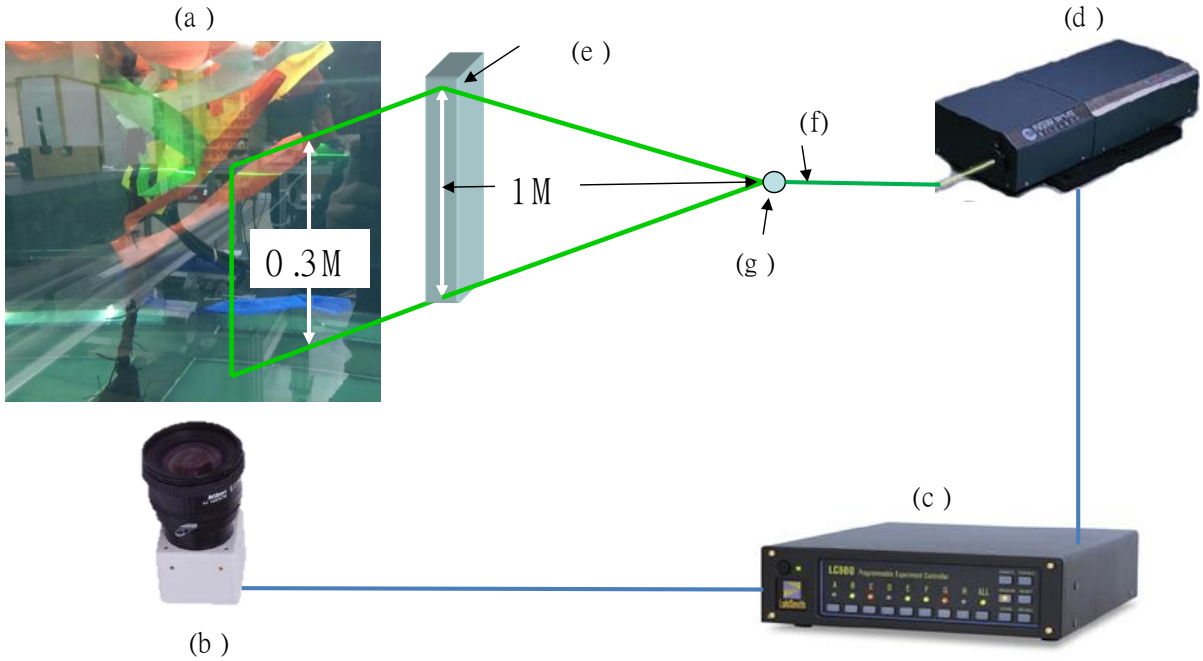

Fig. 1. Experimental set-up for measurements of FAD using PIV (a) FAD measurement area (b) PIV camera (c) PIV controller (d) PIV laser (e) Reflect Optical Mirror (f) Double pulse laser beam (g) Laser splitter.

Table 1. Materials and specifications of net-type and rope-type FADs

	Net-type	Rope-type
Thickness	3 mm	40 mm
Material	PE (Polyethylene)	PE (Polyethylene)
Area	600 mm × 600 mm (Area of net)	1000 mm (Length of rope)
Appearance	50 mm × 50 mm (Length of one side of net knot)	50 mm (Width) × 250 mm (Length) Appearance of a cloth attractor

Table 2. Body length and weight of spindle fish – mackerel (*Scamber japonicus*)

No	Body length (mm)	Body width (mm)	Weight (g)
1	32.5	52.3	620.5
2	31.0	51.2	580.4
3	32.4	56.5	720.5
4	31.6	52.6	620.5
Mean	31.88	53.15	635.5

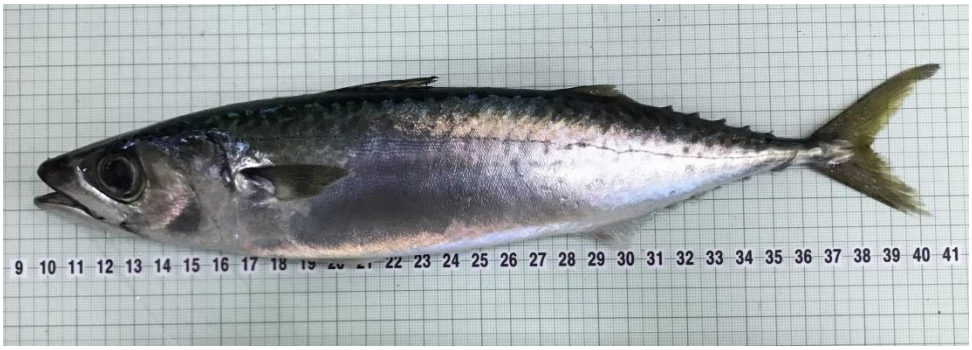

Fig. 2. Spindle fish.

Results and Discussion

Figure 3 shows the results of the velocity and turbulence intensity measured while rotating from 10° to 90° on the central axis to measure the spatial velocity distribution of a net-type entangling FAD, in a circulating water tank with an inlet velocity of 0.504 m/s. The velocity of the existing high-risk net-type entangling FAD increased to 6.85% faster than the inlet velocity from 10° to 40°, and decreased to 3.06% slower from 50° to 90°. The turbulence intensity was 3.77% from 10° to 90°. Considering that the error range of the turbulence in the experimental tank was within 5%, no mechanical difference was detected.

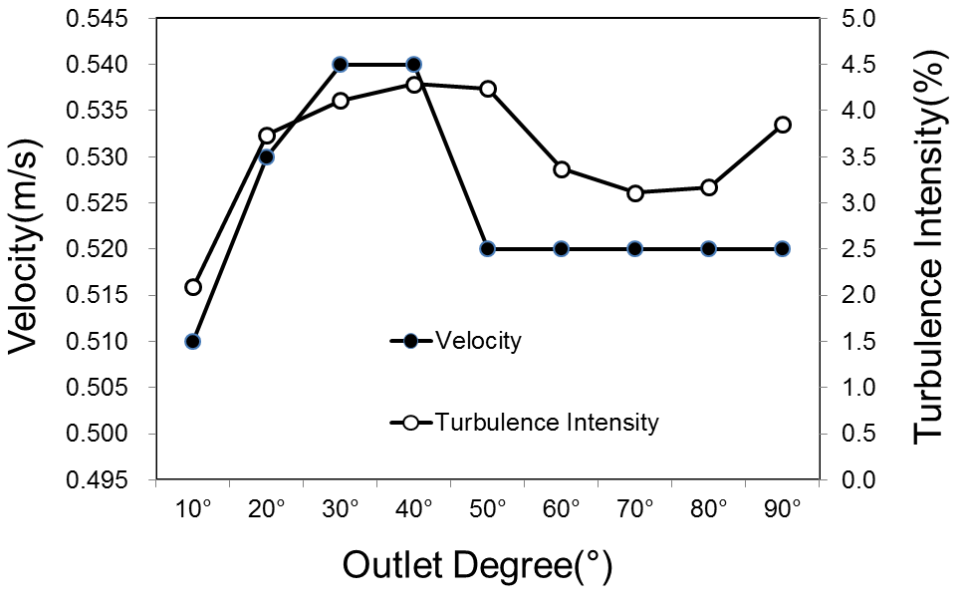

Fig. 3. Velocity and turbulence intensity of net-type FAD using PIV for varying discharge angles.

For the rope-type FAD attached with low-risk cloth attractors, the shape of the cloth attractor differed according to the inlet velocity. Figure 4 shows the velocity and turbulence intensity data for inlet velocities of 0.2 to 0.5 m/s, for which the shape of the cloth attractors on the rope was fully-formed. At an inlet

velocity of 0.2 m/s, when the cloth attractors gradually became horizontal with the direction of the flow, the velocity decreased by 37%. At 0.5 m/s, when the shape was fully horizontal, the difference in the velocity was 44%, indicating that the difference in the velocity increases with increasing velocity. Further, for a turbulence intensity, the increases in the velocity were 37% and 46.9% for inlet velocities of 0.2 and 0.5 m/s, respectively. This indicates that the measured increments were greater than those corresponding to the increases in velocity.

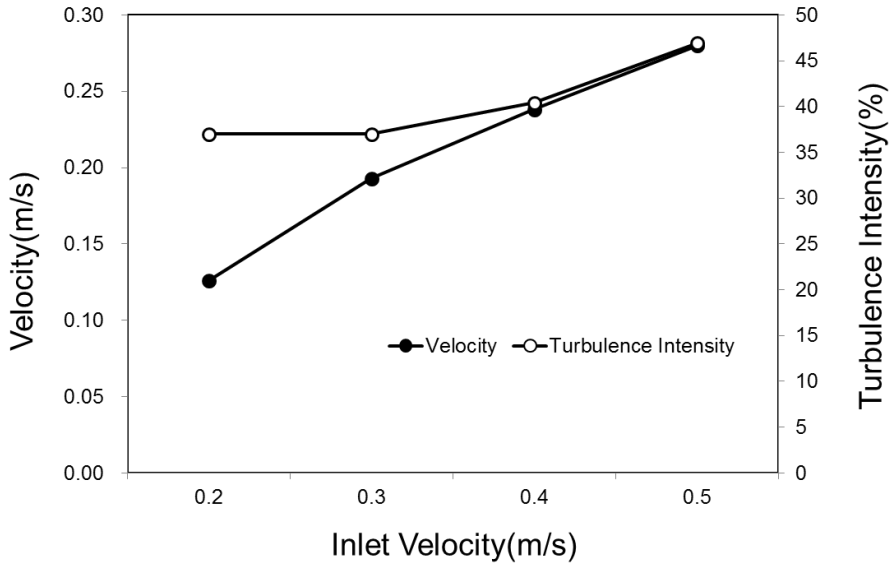

Fig. 4. Velocity and turbulence intensity of rope-type FAD using PIV at different inlet velocities.

At an inlet velocity of 0.504 m/s, at which all the cloth attractors were horizontal with the direction of the flow, the velocity and turbulence intensity data of the net-type FAD are as shown in Figure 5. The standard deviation of the lengthwise velocity for the net-type and rope-type FADs were 0.021 and 0.243 m/s, respectively, indicating that the standard deviation of the rope-type FAD was 1136%. The standard deviation of the turbulence intensity of the net-type

and rope-type FADs were 3.43% and 47.30%, respectively, indicating that the standard deviation of the rope-type FAD was 1380%. Further, the changes of the turbulence intensity were greater than those of the velocity. An analysis of the standard deviation of the lengthwise velocity and turbulence intensity revealed that the rope-type FAD had a higher velocity and the turbulence intensity was comparable to the net-type FAD. This may be due to the effect of fluid stimuli in the block flows, the generation of fluid sounds, and the sheltering of the flows.

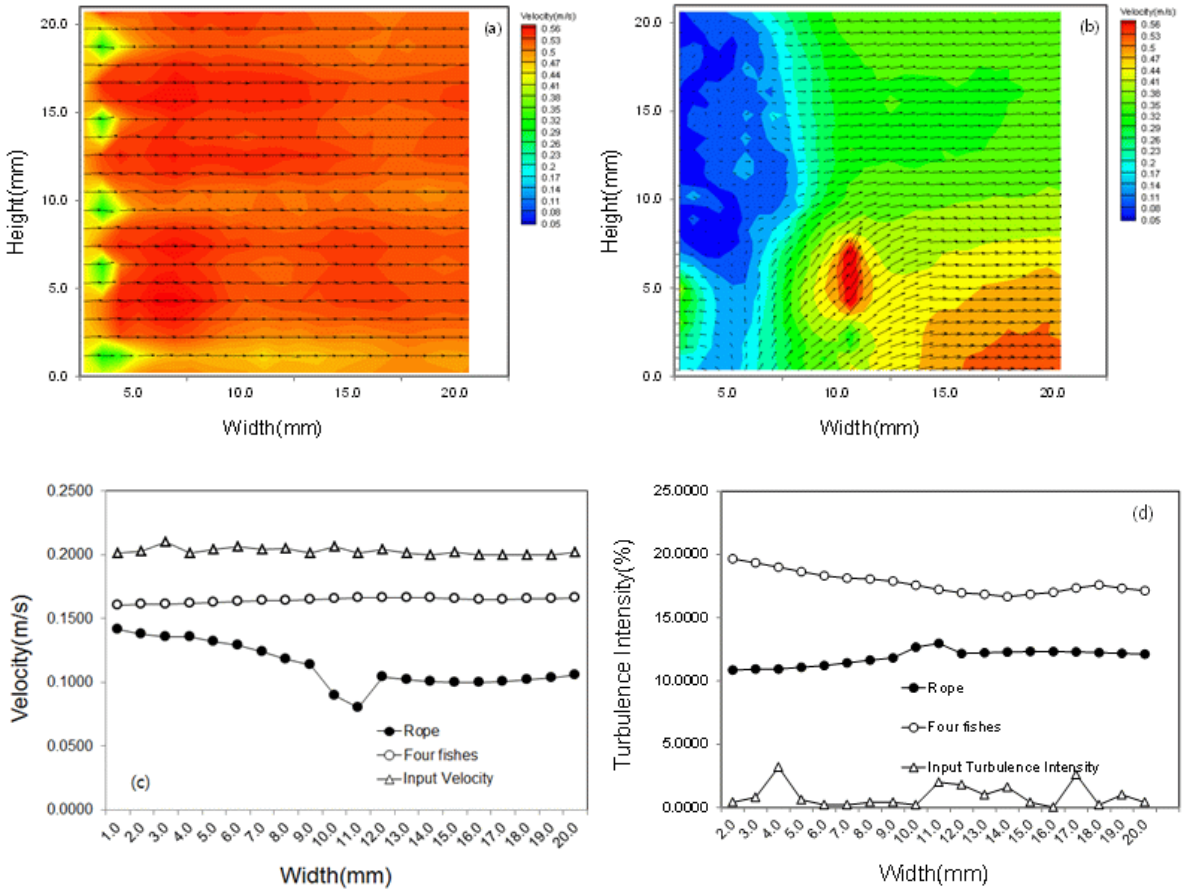

Fig. 5. Measurements of two types of FAD using PIV (a) Net-type FAD Vortex structures (b) Rope-type FAD Vortex structures (c) Velocity distribution by FAD types (d) Turbulence intensity distribution for different FAD types

For an inlet velocity of 0.202 m/s, when the cloth attractors on the ropes start to turn in the direction of the flow, the velocity and turbulence intensity data of the rope-type FAD and four spindle fish are as shown in Figure 6. The standard deviation of the lengthwise velocity of the rope-type FAD and the spindle fish were 0.093 m/s and 0.040 m/s, respectively, where the value of the rope-type FAD changed by 233%. The standard deviation of the turbulence intensity of the rope-type FAD and spindle fish were 10.83% and 16.89% respectively, where the value of the rope-type FAD changed by 64%. The changes for the velocity were greater than those for the turbulence intensity. An analysis of the standard deviation revealed that while there was a significant difference between the rope-type FAD and the spindle fish for the lengthwise velocity, the difference in the turbulence intensity was small. The reason is that the multiple cloth attractors installed onto the rope-type FAD decreased the velocity by artificially blocking the flow, while the swimming of the spindle fish did not disturb the flow. However, the swimming of the fish created a flow structure as complex as the rope-type FAD, which resulted in a similar standard deviation of the turbulence intensity.

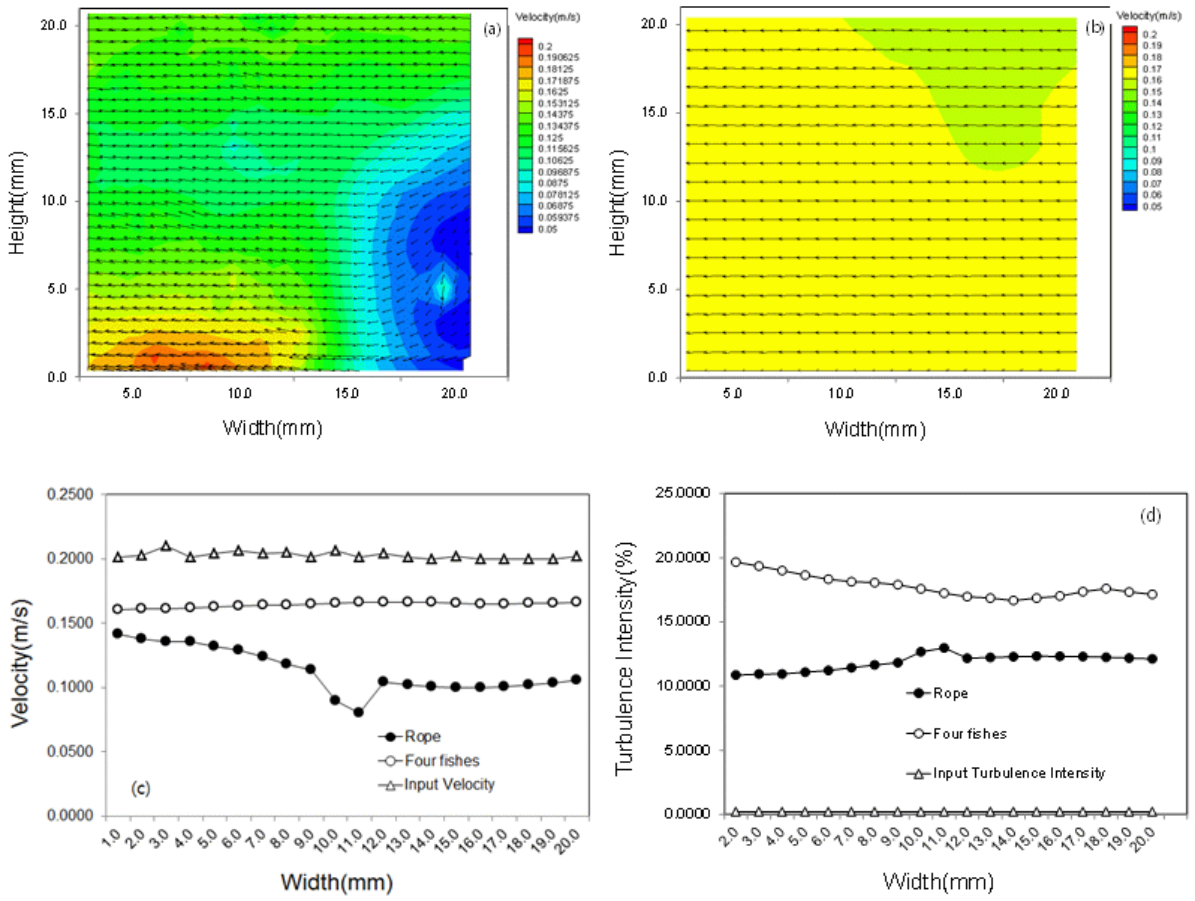

Fig. 6. Measurements of rope-type FAD and spindle-shaped fish using PIV (a) Rope-type FAD vortex structures (b) Vortex structures of spindle fish (c) Velocity distributions of rope-type FAD and spindle fish (d) Turbulence intensity distributions of rope-type FAD and spindle fish.

In this study, the cause of fluid stimuli was quantitatively analyzed using the velocity and turbulence intensity data of high-risk net-type FADs and low-risk rope-type FADs, with respect to the characteristics of how tuna fish gathered (depending on fluid responses), using a flow visualization technique implemented using digital imaging. By modifying the design of the types of knots attached to the rope-type FAD, its fluid hydrodynamic effects, including the block flow function, fluid sound generation, and flow sheltering, using

topographic waves of artificial reefs can be optimized. A more systematic study should be conducted for the same reason.

References

An, H. C., B. S. Bae, K. H. Lee, S. W. Park and J. H. Bae. 2012. Operating performance of hair-tail angling vessel using the LED and Metal halide fishing lamp combination. J Kor Soc Fish Tech, 48, 337-345.

D. Y. MOON, U. K. JANG, J. B. KIM. 1996. Onthe Log-Associated School Fishery of Korean Tuna Purse Seiners. J. Korean Fish. Soc. 29(2), 197-207.

D. Y. MOON, S. J. HWANG, D. H. An, and S. S. KIM. 2007. Bycatch of sharks in Korean tuna longline fishery. J. Kor. Soc. Fish. Tech., 43(4), 329-338.

Jeong Woo Lee. 2000. Future Policy Trend in Artificial Reef Facility Project. Korean Style 12 (1), May 2000, 35-76. pp. 42.

.